Geomechanics and Engineering, *Vol. 38, No. 4 (2024) 335-352*
https://doi.org/10.12989/gae.2024.38.4.335

Effect of wood pellet fly ash on strength and microstructure of Korean weathered granite soil

Jebie A. Balagosa[1a], Min Jy Lee[1b], Yun Wook Choo*[1], Ha Seog Kim[2c] and Jin Man Kim[2d]

[1]*Department of Civil and Environmental Engineering, Kongju National University, 1223-24, Cheonan-daero, Seobuk-gu, Cheonan-si 31080, Republic of Korea*
[2]*Department of Architectural Engineering, Kongju National University, 1223-24, Cheonan-daero, Seobuk-gu, Cheonan-si 31080, Republic of Korea*

(*Received December 25, 2023, Revised July 7, 2024, Accepted July 10, 2024*)

Abstract. Low carbon energy demand in South Korea is increasing, hence leading to an increasing usage of wood pellets and the amount of its combustion by-product called wood pellet fly ash (WA). In an effort to develop recycling technology, this research investigates the use of WA as a new sustainable binder for backfill soil materials. The influence of WA on weathered granite soils (WS) is investigated by mixing 5%, 15%, and 25% of WA dosage, compacted at optimum moisture content, then cured for 3, 7, 14, and 28 days. After curing, the compacted specimens were investigated through unconfined compressive tests, pH tests, total suction tests, and microstructural analysis. The findings suggest that the higher the dosage rate, the higher strength and modulus. Additionally, the alkali ions of WA aid in the cementation of WS particles, and newly cementitious minerals are confirmed after 28 curing days. The refinement of pore microstructures led to a denser WS matrix and stiffness improvements. The results validate the binding potential of wood pellet fly ash on weathered granite soils in terms of strength, modulus, and microstructures.

Keywords: microstructural analysis; sustainable binder; unconfined compressive tests; weathered granite soils; wood pellet fly ash

1. Introduction

The deleterious effects of climate change have pushed the international community to shift away from traditional fossil fuels and promoted the use of alternative and renewable energy sources to reduce greenhouse gas emissions (Nunes *et al.* 2014). Biomass-based energy products are seen as an efficient alternative to coal due to its lower carbon content than fossil fuels (Abbasi and Abbasi 2010). One good candidate is wood pellet energy production and its global trend is increasing due to their wide range of applicability such as residential, commercial properties, and power plant industries (International Organization for Standardization (ISO), 2021). In line with this international trend, South Korea developed energy policies (Ministry of Trade Industry and Energy 2017a, 2017b) indicating the need to convert existing coal-fired power plants into renewable energy plants using wood pellet fuel (Kim *et al.* 2021a). As a result, the country's demand for wood pellets surged (Oh *et al.* 2014, Wood Resources International 2017, Proskurina *et al.* 2019) and are anticipated to progressively increase (Hawkins Wright 2017). This led to the increase in its by-products wood pellet fly ash (WA), which are typically stored in landfill repositories. To remediate the possible saturation of WA repositories, recycling technology for WA is necessary.

Chemical soil stabilization is an essential technique that improves the physical characteristics of problematic soils, including soft soils (Bagherinia and Zaimoğlu 2021, Horpibulsuk *et al.* 2013, Mekonnen *et al.* 2022, Gidebo *et al.* 2023) and weathered granite soils (Burke *et al.* 2007, Opukumo *et al.* 2022, Balagosa *et al.* 2024). This method improves soil mechanical properties (i.e., strength, compressibility, durability, water resistance, settlement, liquefaction, etc.) by adding binding materials such as cement, lime, fly ash, and chemical polymers (Dayioglu *et al.* 2017; Bagherinia and Işik 2022, Yi *et al.* 2016, Chang *et al.* 2015, Ale 2023, Zivari *et al.* 2023, Regasa *et al.* 2023).

Recycling industrial by-products, including biomass ash, has gained traction due to the need of eco-friendly and new sustainable soil binder material (Liu *et al.* 2022). The use of these binders primarily aims to reduce the carbon emission produced when using conventional soil stabilizers: i.e., cement, lime, or other chemical additives (Ali *et al.* 1992, Holm 2003, Farnsworth *et al.* 2008, Roy 2014).

Examples of biomass ash by-products that were previously explored for ground improvement applications are wastes discharged from power plants (Mácsik *et al.* 2012, Bohrn and Stampfer 2014, Vanhanen *et al.* 2014), and industrial manufacturing (Okagbue 2007, Ayininuola and Oyedemi 2013). Biomass ash mixed soils were found

*Corresponding author, Professor
E-mail: ywchoo@kongju.ac.kr
[a]Ph.D., Postdoctoral Researcher
[b]Ph.D. Student
[c]Ph.D., Research Professor
[d]Ph.D., Professor

Copyright © 2024 Techno-Press, Ltd.

ISSN: 2005-307X (Print), 2092-6219 (Online)

Table 1 Summary of the specimen preparations and chemical constituents of biomass ash used for soil stabilization

Biomass Ash Waste and Host Soil	SiO_2	Al_2O_3	CaO	Fe_2O_3	MgO	SO_3	K_2O	Na_2O	P_2O_5	LOI	Specimen Preparations	Unconfined compressive strength (q_u)	Reference
Wood Pellet Fly Ash + WS	23.30	6.60	27.80	3.80	3.20	8.40	16.60	3.50	2.30	6.82	SC: up to 25%* OMC: 9.6% to 12% MDD: 1.90 to 1.93 g/cm^3 CD: 3, 7, 14, and 28 days$^+$	0.21 – 2.10 MPa	Present Study
SDA + RAP	6.60	-	33.40	1.10	4.80	4.10	27.50	-	3.90	22.00	SC: up to 12.5%* OMC: 15.2% to 27.2% MDD: 1.47 to 1.74 g/cm^3 CD: 1 day$^{\wedge\#}$	-	Osinubi *et al.* (2012)
SDA + LS	85.00	2.70	3.50	1.70	0.30	-	-	-	0.40	4.30	SC: up to 10%* OMC: 19% to 28% MDD: 1.84 to 1.87 g/cm^3 CD: 7 days$^\#$	0.65 – 1.85 MPa	Otoko and Honest (2014)
SDA + CS	83.60	2.60	3.60	1.80	0.30	-	0.50	0.20	-	-	SC: up to 12%* OMC: 13.2 to 25.7% MDD: 1.37 to 1.55 g/cm^3 CD: 7 days$^\#$	0.18 – 0.31 MPa	Butt *et al.* (2016)
SDA + SS	83.60	0.40	14.20	0.60	-	-	0.50	0.20	-	-	SC: cement + SDA (1:2) and up to 10.0%* OMC: 14.1% MDD: 1.72 g/cm^3 CD: 7$^\#$, 30, 60, 90 days	0.09 – 0.23 MPa	Ojuri and Epe (2016)
RHA + CS	67.30	4.90	1.40	0.90	1.80	-	-	-	-	17.70	SC: up to 12.0%* OMC: 16.5% to 28.1% MDD: 1.38 to 1.48 g/cm^3 CD: 6 day$^\wedge$, 1 day$^\#$	0.20 – 0.29 MPa	Alhassan (2008)
SWA + LS	24.53	-	29.05	0.58	7.03	-	16.24	19.02	-	-	SC: up to 15%* OMC: 13.3% to 14.8% MDD: 1.80 to 1.90 g/cm^3 CD: -	-	Ayininuola and Oyedemi (2013)
Wood Ash + CS	24.50	-	29.10	0.60	7.00	-	16.20	19.00	-	-	SC: up to 15%* OMC: 12.9% to 23.2% MDD: 1.54 to 1.82 g/cm^3 CD: 28 days$^{\#\wedge}$	0.07 – 0.17 MPa	Okagbue (2007)
Wood Ash + CS	25.80	14.70	29.80	0.90	5.30	0.70	9.60	7.50	2.30	2.70	SC: up to 12.5%* OMC: 23% to 28% MDD: 1.46 to 1.55 g/cm^3 CD: -	0.06 – 0.15 MPa	Nath *et al.* (2018)
Wood Ash + SS	47.60	7.90	24.70	1.30	3.20	8.30	4.90	1.20	-	5.10	SC: up to 20%* OMC: 7% MDD: 1.79 g/cm^3 CD: 4 days$^\#$, 7 days$^\wedge$	-	Skels *et al.* (2016)

Note: Chemical constituents and LOI are in %; - = details were not provided; + = sealed & water-bath curing; # = soaked curing; ^ = unsoaked curing; * = Biomass Ash Stabilizer dosage by dry weight of soil; SDA = Saw dust ash; RHA = Rice husk ash; SWA = Softwood ash; WS = Weathered granite soils; RAP = Reclaimed Asphalt Pavement; LS = Lateritic Soils; SS = Sandy Soils; ES = Expansive Soil; CS = Clayey Soils; SC = Stabilizer contents; OMC = Optimum moisture contents; MDD = Maximum dry density; CD = Curing days

to improve mechanical properties and revealed a unique strength gain based on the biomass ash binder type and dosage rate, water-binder ratio, sample preparations, compaction characteristics, soil type, and curing conditions (Okagbue 2007, Alhassan 2008, Osinubi *et al.* 2012, Ayininuola and Oyedemi 2013, Otoko and Honest 2014, Butt *et al.* 2016, Ojuri and Epe 2016, Šķēls *et al.* 2016, Nath *et al.* 2018). The previous research exhibited the soil-biomass ash binding potential through their strength gain relative to the production of new cementitious minerals (Okagbue 2007, Cherian and Siddiqua 2021). Also, the biomass ash binding potential can be chemically activated through the presence of moisture (Ali *et al.* 1992, Basha *et al.* 2005, Sabat and Nanda 2011) and its unique chemical constituents, as presented in Table 1. Interestingly, the components of WA in this study also contain calcium oxide (CaO) and silica dioxide (SiO_2), which points to the possibility that it could promote pozzolanic reaction and form cementitious products.

Previous studies have reported a change in mineral composition between raw and hardened WA when mixed with water (Kim *et al.* 2022, Kim *et al.* 2021c, Kim *et al.* 2021b). Initially, WA consists mainly of quartz and lime, while the hardened form shows low peaks of new hydrocalumite hydrate through X-ray diffraction tests. The low peak intensity of hydrocalumite mineral suggests its minimal strength contribution. Nevertheless, these findings suggest unique hydraulic properties of WA. On top of that, the WA contains quite plenty of K, Na, Ca, Fe, and Mg, which is beneficial in supplying alkali ions to stimulate the cementation process. Notably, most previous studies in soil stabilization have focused on clean sands and clay soils. There is currently no study that investigates the stabilizing mechanism of pure wood pellet fly ash to weathered granite soils (WS).

This study primarily aims to evaluate the stabilizing mechanism of WA as a sustainable binder without additional cement compounds for WS as an alternative backfill materials. Specifically, this study investigated the following:

1. Influence of WA on the mechanical properties of WS at unsaturated conditions (at 5%, 15%, and 25% WA by dry mass of soil),

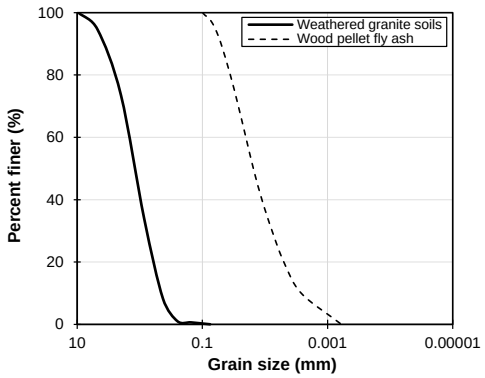

Fig. 1 Particle size distributions of weathered granite soil (sieve analysis) and wood pellet fly ash (laser diffraction particle size analyzer using Shimadzu SALD-2300)

2. Investigate the production of cementitious minerals on WA-WS surface and microstructures for up to 28 days,
3. Examine the role of WA on the cementation and suction, and
4. Develop a model equation that shows the relationships between unconfined compressive strength (q_u), wood pellet fly ash contents, over 28 curing days.

2. Testing materials and methods

WS are used as a natural host soil and are commonly found in the mountainous sites of South Korea. This WS is classified as Material Type 2 according to AASHTO Transportation Officials, (1993), classified as poorly graded sands (SP) by the Unified Soil Classification System (USCS) (ASTM D2487, 2020). On the other hand, the WA used in this study were originally in the form of wood pellets and imported from Southeast Asian countries, which Vietnam and Thailand predominantly produce. These pellets undergo combustion at Yeongdong Eco Power Plants operated by Korea South-East Power Co. Ltd. (KOEN) to generate electricity. Subsequently, the wood pellet fly ash was produced after combustion and discharged through a hybrid dust electric precipitator that collects by-products through the bag filters located on the top of the boiler. Fig. 1 presents the particle size distribution of WS and WA exhibiting median particle size (D_{50}) of 1.21 mm (ASTM D6913, 2017) and 0.015 mm (through laser diffraction), respectively. The unique size of WA exhibit potential as a new type of biomass fly ash (BFA) construction materials. These ashes have a typical particle size of 0.004 to 0.1mm (Šķēls *et al.* 2016, Anupam *et al.* 2013, Maeda *et al.* 2017, Wang *et al.* 2012). The small particle size of BFA promotes increase in hydration reactivity due to their larger surface area (Barbosa and Cordeiro 2021). Notably, BFA can be considered as a cost-effective solution when utilize as a binder since pre-processing of the raw materials is not required (Fořt *et al.* 2021, Sarkkinen *et al.* 2018). WA is typically dark gray with a dry density of 2.31g/cm^3, fineness of 3350 cm^2/g, and pH of 12 or higher. Table 2 summarizes their index properties.

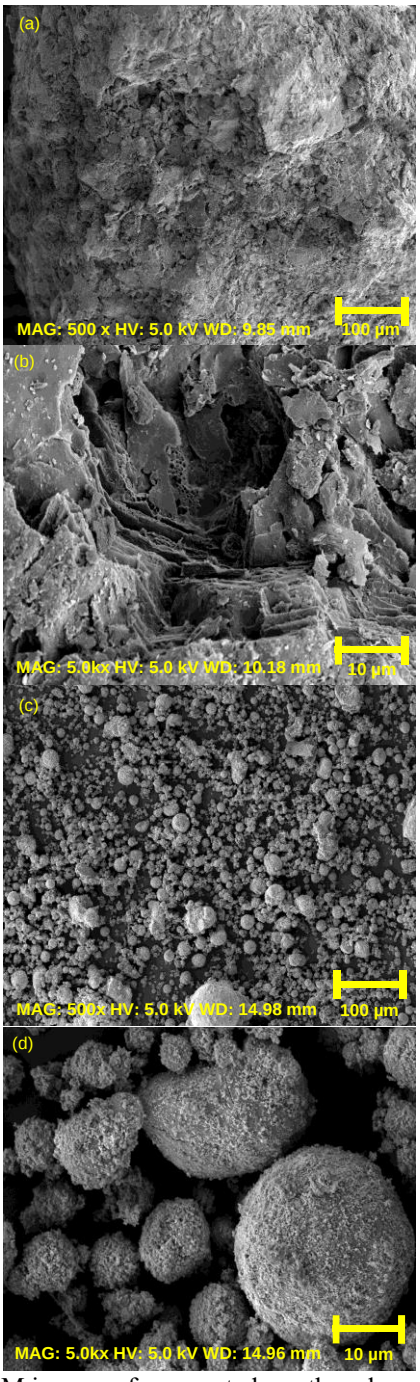

Fig. 2 SEM images of compacted weathered granite soils: (a) 100 µm, and (b) 10 µm; wood pellet fly ash at (c) 100 µm, and (d) 10 µm

Fig. 2 displays the particle morphologies of WS and WA produced by scanning electron microscope (SEM). The WS grains have mainly sub-angular shapes, while WA has smaller particle size, lower sphericity, larger surface areas, and higher porosity. The lower specific gravity and higher specific surface depict the porous structures of WA grains. These physical features exhibit hydrophilic and water absorption potential, which promotes capillary action through simultaneous hydration of oxides (Grau *et al.* 2015). Subsequently, when WA is compared with previous sustainable soil binders such as biomass ash (Table 1), by-

Table 2 Geotechnical properties of host soil and wood pellet fly ash

Properties	Weathered Soil	Wood Pellet Fly Ash
Specific gravity, G_s	2.67	2.30
Maximum void ratio, e_{max}	1.02	-
Minimum void ratio, e_{min}	0.55	-
Grain size (mm)	d_{10} = 0.45	$d_{10} = 2.64\times 10^{-3}$
	d_{30} = 0.78	$d_{30} = 7.89\times 10^{-3}$
	d_{50} = 1.21	$d_{50} = 15.35\times 10^{-3}$
	D_{60} = 1.49	$d_{60} = 20.23\times 10^{-3}$
C_u	3.34	7.68
C_c	0.91	1.17
Passing no.4 sieve (%)	94.64	100.00
Passing no. 200 sieve	0.01	97.10
Soil Classification, USCS	SP	-
Plastic Index, PI (%)	NP	-
Optimum moisture content* (%)	11	-
Maximum dry density* (g/cm^3)	1.98	-

Note: *Modified proctor test (ASTM D1557-12e1)

Table 3 Testing conditions of specimens

Specimen ID	R_c (%)	Specimen ID	R_c (%)	Specimen ID	R_c (%)	Specimen ID	R_c (%)	Specimen ID	R_c (%)
WA5-C3-1	Fail	WA5-C14-3$^{\#}$	Fail	WA15-C7-1	97.00	WA15-C28-3$^{\#}$	94.50	WA25-C14-2	95.40
WA5-C3-2	Fail	WA5-C14-4*	Fail	WA15-C7-2	96.30	WA15-C28-4**	94.60	WA25-C14-3$^{\#}$	95.90
WA5-C3-3$^{\#}$	Fail	WA5-C28-1	96.10	WA15-C7-3$^{\#}$	95.80	WA25-C3-1	95.10	WA25-C14-4*	95.60
WA5-C3-4*	Fail	WA5-C28-2	95.40	WA15-C7-4**	95.60	WA25-C3-2	94.70	WA25-C28-1	94.60
WA5-C7-1	Fail	WA5-C28-3$^{\#}$	94.50	WA15-C14-1	97.90	WA25-C3-3$^{\#}$	94.50	WA25-C28-2	95.20
WA5-C7-2	Fail	WA5-C28-4**	95.80	WA15-C14-2	96.70	WA25-C3-4*	94.90	WA25-C28-3$^{\#\dagger}$	96.30
WA5-C7-3$^{\#}$	Fail	WA15-C3-1	95.30	WA15-C14-3$^{\#}$	95.80	WA25-C7-1	95.90	WA25-C28-4**	96.20
WA5-C7-4*	Fail	WA15-C3-2	94.70	WA15-C14-4*	95.40	WA25-C7-2	94.80		
WA5-C14-1	Fail	WA15-C3-3$^{\#}$	94.50	WA15-C28-1	96.10	WA25-C7-3$^{\#}$	94.50		
WA5-C14-2	Fail	WA15-C3-4*	94.80	WA15-C28-2	95.40	WA25-C7-4**	95.70		
WS-1	96.00	WS-2	96.90	WS-3	95.90	WA25-C14-1	96.50		

Note: WA = wood pellet fly ash, and the subsequent number is the dosage defined as a dry mass ratio of WA to WS; C and the following number is the curing and testing day; Last number in specimen ID is the testing sequence; $^{\#}$ = after UCT tests specimens subjected also for pH tests; ** = series 2 specimens subjected for both pH test and total suction tests; * = series 1 specimens subjected for pH tests only; † = specimen tested by XRD, SEM and EDS; Fail = fail to extract specimens and no suction test (water contents are measured after mold extraction); R_c = relative compaction; Compacted WS specimens were tested immediately after compaction

product fly ash (SiO_2 over 50%) (Bhatt *et al.* 2019), and high calcium fly ash (Behnood 2018), WA has SiO_2 and CaO content of less than 30% and high alkaline components (K_2O, Na_2O, and MgO). Interestingly, the combined proportions of WA's SiO_2, CaO, and alkali constituents are indicative of its binding potential (Kim *et al.* 2022, Kim *et al.* 2021c, Kim *et al.* 2021b), as shown in the strength gain of biomass ash mixed soils (Table 1). Furthermore, the low SiO_2 content in WA suggests low pozzolanic reactivity (Greenberg 1961, Edil *et al.* 2006).

Fig. 3 illustrates the specimen preparation on WA mixed WS. Multiple samples of WS were combined with 5%, 15%, and 25% WA (defined as a dry mass ratio of WA to WS) by dry mixing method. In practice, this method aligns to dry-mixing techniques for soil stabilization (Timoney *et al.* 2012, Wang *et al.* 2022). The WA dosage range of 5% to 25% (measured by the ratio of WA powder to total dry mass of soil) utilized in this study is practically selected based on the typical range applied on treated soil-based structures (Šķēls *et al.* 2016, Lorenzo and Bergado 2006, Madhyannapu *et al.* 2010), for economic purposes (Davidson, 1961) and as a base material for comparing the strength change of soil columns mixed with WA blended binders (mixture of cement, ground granulated blast furnace slag, and WA) performed in a separate project. After preparing the material proportions, WS was oven dried for 24 hours and then sieved using sieve number 5 (9.5 mm

(a) Preparation of WS and WA portions: 5%, 15%, and 25% (by dry mass of soil)

(b) Mixing of moist WS and dry WA

(c) Compacted specimens inside mold

(d) Sealed curing chamber with small amount of water inside

(e) Extracted specimens: 5% WA-WS, 15% WA-WS, and 25% WA-WS

Fig. 3 Specimen manufacturing process.

opening). Prior mixing, pure WS grains were firstly homogenized thoroughly and mixed at estimated water contents using a laboratory mixer for one-and-half to two minutes. Next, dry WA powder was mixed thoroughly with the moist soil until homogenized for eight mins, then modified proctor test (ASTM D1557, 2012) is performed.

The measured maximum dry density (MDD) and optimum moisture content (OMC) were utilized as the mix proportions for the cylindrical specimens, following the similar mixing procedure for the treated soils used in modified proctor tests. After mixing, the specimens were compacted inside a cylindrical split mold (50-mm-diameter and 100 mm tall), and a total of five layers were employed using an 8-mm-diameter tamping rod, targeting relative compaction (R_c) of 95% at the OMC. Table 3 summarizes the testing condition and compaction characteristics of WA mixed soils. The specimen molds were sealed with a plastic sheet to reduce moisture loss over 28 curing days (Ho *et al.* 2017) and cured at room temperature (25±1°C) in a closed tank partially filled with water (without direct contact with water). The humidity inside the curing chamber is maintained at 85±2% (measured using a humidity meter) to ensure the specimens would not dry out. While previous studies indicate that curing at elevated temperatures enhances the time period of the maximum mobilized strength of soils mixed with by-product materials (Narmluk and Nawa 2014, Sukprasert *et al.* 2021, Sukmak *et al.* 2019). This study focuses on the WA strength mobilization to WS and simulating backfilling process through dumping, compacting, and curing at normal field temperatures above the water table. The effects of high temperatures on WA's binding capacity in WS are beyond the scope and require further investigation.

A total of 36 specimens were cured at 3, 7, 14, and 28 days (triplicate specimens per curing day). After each curing day, the specimens were extracted from the molds then unconfined compressive tests (UCT) were performed with a 1%/min vertical displacement rate (ASTM D2166, 2016) to determine the unconfined compressive strength (q_u) and secant modulus (E_{50}). Then, the fractures from the strongest specimen (after UCT tests conducted at 28 days) were fragmented for a series of SEM-EDS and XRD tests. These fractures were carefully trimmed to match the dimensions of the mold for SEM-EDS testing (using Model MIRA LMH) performed at voltages ranging from 5 to 20 kV with a resolution of 1 nm. Qualitative X-ray diffraction (XRD) test was performed (using a Rigaku Mini-Flex600 XRD instrument) and operated at 40 kV and 30 mA, with a Cu target (obvious peaks in the 2θ region of 0 to 5 were not detected, therefore the analysis focuses on the 2θ range of 5 to 70) to analyze the reflected mineral peaks and intensities of mixed soils. The purpose of these tests was to confirm

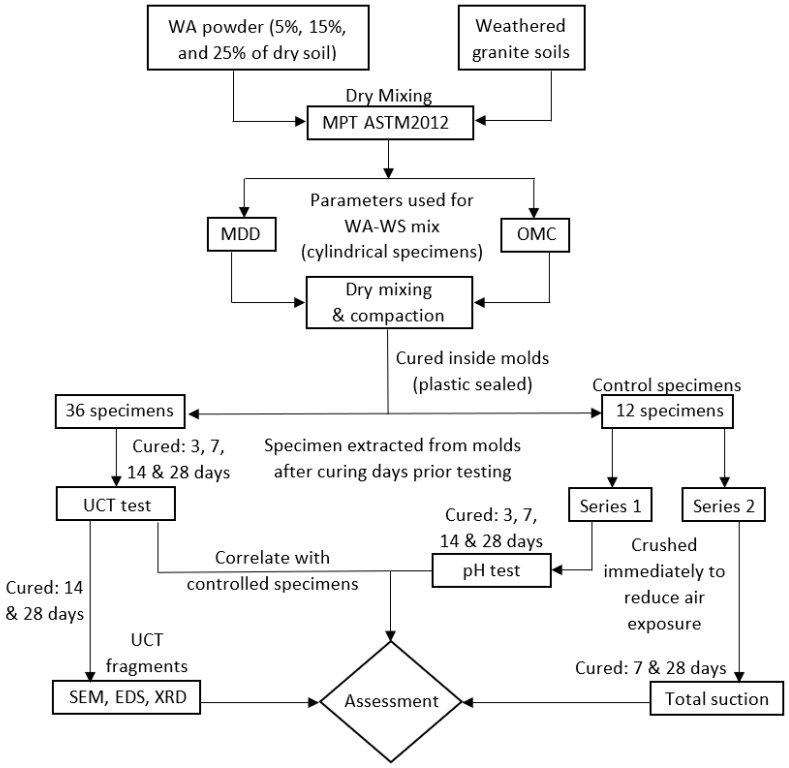

Fig. 4 Testing plan flow chart for the testing plans in evaluating the mechanical properties of wood pellet fly ash stabilized weathered granite soils

the influence of WA on the WS microstructural shape, size, and chemical change through the presence of new cementitious materials.

In addition, twelve extra WA-WS samples were created and cured for 3, 7, 14, and 28 days (same compaction characteristics and curing conditions as those tested in UCT). These samples then served as controls for two sets of tests: Series 1 (marked with "*" in Table 3), involved pH tests (ASTM D5239, 2012), and Series 2 (marked with "**" in Table 3) involved total suction and pH tests. After curing period, the specimens were promptly removed from the molds to minimize air exposure. The central cores of the specimens were then split into three sections: upper, middle, and lower. These sections were carefully sliced into smaller intact specimens measuring around 9 mm and smaller. Series 1 testing was conducted on the intact WA mixed soil samples with distilled water (proportions of 1:5), and the average pH value from the three sections was calculated. For Series 2, the remaining samples were immediately gathered to preserve the original material conditions and transferred to the aluminum caps to assess the total suction using a potentiometer (WP4C, METER Group), water content, and pH tests. The use of WP4C was successfully employed to rapidly monitor total suction on sliced fractures at higher suction condition (Ferrari *et al.* 2013, Muguda *et al.* 2017, Murray and Tarantino 2019, Das *et al.* 2022) to assess the hydraulic behaviour of unsaturated soils (Ponzoni *et al.* 2021, Yuan *et al.* 2021) and stabilized soils (Muguda *et al.* 2017, Almajed *et al.* 2023, Balagosa *et al.* 2023). The summary of the testing program, mix proportions, and curing days are illustrated in Fig. 4.

3. Results

3.1 Compaction properties

Fig. 5 plots the change of the MDD and OMC of WA-WS mixtures, and the achieved molding densities of the cylindrical specimens, zero and 20% air void (A_V) lines for WS (G_s = 2.67) were also included as a reference. As WA contents increase, the MDD and OMC decrease. This result leads to the position of the compaction curves to shift left and downward. In particular, the OMC of 5% WA-WS accounts for the highest OMC and is linked to the biomass ash's hydrophilic nature (Etiégni and Campbell 1991, Misra *et al.* 1993, Okagbue 2007, Ayininuola and Oyedemi 2013, Mimini *et al.* 2019, Yuan *et al.* 2021). On the other hand, the slight decrease in the OMC of 15% and 25% WA-WS suggests early binding characteristics of wood pellet fly ash (due to initial WA coating) and increase.

3.2 Unconfined compressive strength and secant modulus

Fig. 6 presents the effect of WA contents on the change of q_u and w_c of WA-WS over 28 curing days. The q_u increases as the WA content increase up to 14 days, then subsequently decrease for 28 days. In particular, the 28-day q_u of 5% WA specimen ranges from 0.2 to 0.3 MPa, almost identical to the q_u of WS having 0.19 to 0.32 MPa. This finding suggests that early-day cementation cannot be achieved due to the premature binding of 5% WA on WS.

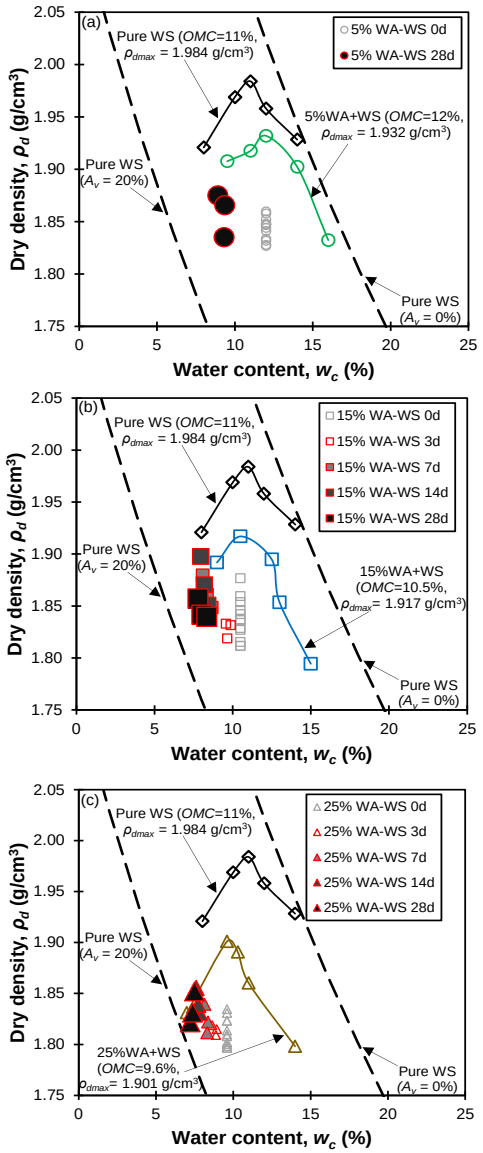

Fig. 5 Modified proctor test result on WS with WA, and the change of ρ_d and w_c of the tested specimens over curing days: (a) 5% WA-WS, (b) 15% WA-WS, and (c) 25% WA-WS

The 15% WA treated specimen has a q_u of 0.35 to 1.4 MPa, while the 25% WA-WS q_u ranges from 0.59 MPa to 2.1 MPa. Notably, the 28-day q_u of 15% and 25% WA-WS were slightly lower and similar to their 14-day q_u. These findings suggest slow strength gain and variations in WA hydrate production owing to the wide range of WS particles size (Fig. 1) and the uneven distribution of water (OMC) to WA particles in the soil grains. On the other hand, the 7-day wc for the 15% and 25% WA-WS were nearly identical (w_c ranges from 8.08% to 8.66%). Then at 28 days, the average w_c reduction from the molding water contents ($w_{c(m)}$) of 5%, 15%, and 25% WA specimens is 2.83%, 2.54%, and 2.30%, respectively. The measured strength increase and w_c reduction suggest WA's hydration potential through the binder's consumption of water particles (Kim *et al.* 2022, Kim *et al.* 2021c, Kim *et al.* 2021b) and reveals WA's

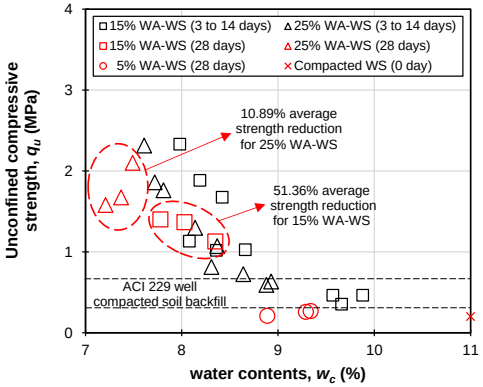

Fig. 6 Effects of wood pellet fly ash contents on the change of q_u and w_c of WA-WS samples over curing days

hydration reactivity (due to its larger surface area) with the soil grains over 28 curing days. Furthermore, the measured 28-day $w_{c(m)}$ reductions of almost 3% may be used as a contributor in strength monitoring for WA-WS compacted at OMC and MDD.

The increase in WA dosage rate shows coupled effects on water desorption and retention in the unsaturated WA-WS matrix. These findings suggest alteration on WS particle contacts due to the variation of retaining water between the modified pore structures inside the WA-WS matrix. It is noteworthy, that the early stage of binder hydration influence development of initial stiffness and mechanical properties of cementitious soils (Jing *et al.* 2022, Phan *et al.* 2021). In this study, the hydration characteristic of WA is considered as the alkali activation of WA with soil minerals. The detailed WA's stabilization mechanism of 15% and 25% WA-WS will be further discussed in Section 4.1.

The measured q_u-gain of WA-WS suggests that it is possible to mobilize 90% of peak strength even under ambient conditions. Previous studies on low calcium fly ash mixtures suggest that increased temperatures can help accelerate cementation (Narmluk and Nawa 2014, Sukprasert *et al.* 2021, Sukmak *et al.* 2019). Hence, these findings imply that strength mobilization of by-product fly ash mix varies with temperatures. However, this study focuses on the WA strength mobilization to WS and simulating backfilling process through dumping, compacting, curing at normal temperatures in the field, the change of WA's binding capacity at high temperatures is beyond the scope, and further studies are needed. The measured q_u of 15%- and 25%-WA-stabilized weathered soils (3 to 28 days cured) satisfies the strength requirement for National Ready Mixed Concrete Association (NRMCA) for backfill materials ranging between 0.3 MPa to 0.7 MPa. These backfill materials can be used for trenches, utility lines, filling material for underground cavity remediation, and are ideal for areas subjected to future excavations using conventional digging equipment (ACI Committee 229, 1994, Ma *et al.* 2020). These types of backfill materials are not subjected to large loads or stresses; thus, high strength requirements are not required. All WA-stabilized soil demonstrated a 1.3 to 5.52 increase in q_u than those of unstabilized compacted WS.

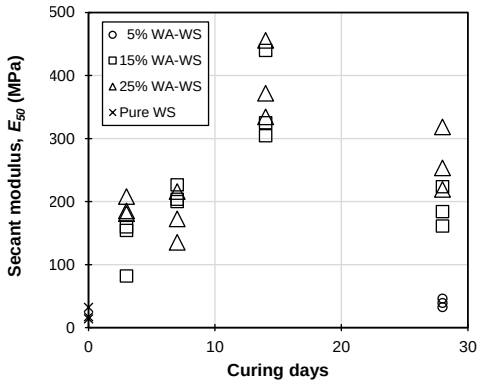

Fig. 7 Effects of wood pellet fly ash contents on the E_{50} of WA-WS samples over curing days

Fig. 7 plots the E_{50} of the WA-treated WS over 3 to 28 curing days. The modulus increases with the increase in WA dosage and follows a similar trend of the q_u profile. The 28-day E_{50} of the 5%-WA specimens achieved 32.5 to 46.21 MPa. The 15%-WA-treated specimens E_{50} range from 82.03 to 223.72 MPa. While the 25%-WA specimens have E_{50}, ranging from 180.88 MPa to 318.88 MPa. These results confirms that WA-WS forms dense soil structure since their E_{50} exceeds 30 to 35 MPa (Bohrn and Stampfer 2014, Obrzud and Truty 2018).

3.3 Effect of WA's cementation on dry density and failure strains

The contribution of WA's cementation in WS is also corroborated with the increase of ρ_d of the tested specimens (as shown in Fig. 4). The average increase of the 7-day ρ_d of 15% and 25% WA-WS are 0.86% and 0.94%, respectively, compared to their molding ρ_d. Then after 28 days, the average increase of ρ_d for 5%, 15%, and 25% WA-WS are 0.86%, 1.01%, and 1.21%, respectively. These findings reveal that as curing days increase, the position of the ρ_d shifted left and upward due to gradual consumption of water particles (through WA hydration) and production of new mineral formations which enhanced the particle contacts of WA-WS matrix.

Fig. 8 presents the influence of the change of ε_f on q_u of WA-WS as curing days increase. All treated WS showed improvement on the soil structure exhibiting a hardening behaviour due to a measured very small strains of less than 1% at axial failure. The 7-day ε_f of 15% WA-WS ranges from 0.59% to 0.67%, whereas the 25% WA-WS were measured at 0.69% to 0.76%. Subsequently, the measured 14 and 28-day ε_f of 15% were almost identical, suggesting no improvements in the stiffness, while the 25% WA-WS exhibits a slight decrease of 28-day ε_f. These findings imply that the stiffness between WA-WS particles strongly increased as WA content increased. Thus, the failure strains are a function of WA cementation.

3.4 pH Tests

Fig. 9(a) illustrates the decrease of pH values as curing days increase. In particular, the pH of 5% WA specimens

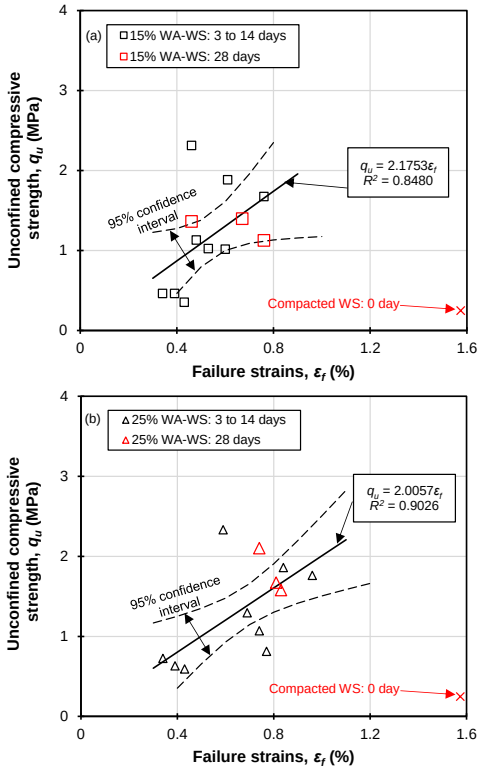

Fig. 8 Correlation between ε_f and q_u: (a) 15% WA-WS, and (b) 25% WA-WS

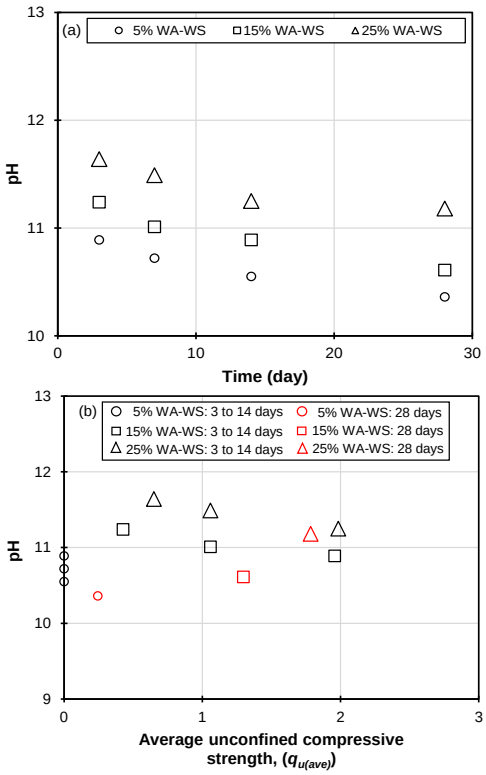

Fig. 9 Effects of WA contents and curing days on (a) measured pH, and (b) pH-$q_{u(ave)}$ relationship

achieved 10.89 to 10.36 for 3 to 28 curing days. The 15% WA-treated specimen has a pH of 11.24 to 10.61. While the 25% WA content presents the highest pH, ranging from

11.64 to 11.18 over 28 curing days. The reduction of pH values indicates the consumption of alkali ions for cementation. Fig. 9(b) presents the relationship between pH and average unconfined compressive strength ($q_{u(ave)}$) for 28 days. No clear correlation for all WA-WS specimens. These findings are analogous to the nonlinear behaviour between the increasing WA content and q_u over 28 days (Fig. 6). Hence, the association of pH with WA dosage rate (*WADR* is the ratio of dry WA to dry soil mass in %), curing days (*CD*), and $q_{u(ave)}$, were then assessed through Spearman's rank correlation coefficient (*rho*), Pearson correlation coefficient (R) (Cohen 1988) with their corresponding significance value (p).

A strong positive, statistically significant association between pH-*WADR* is indicated by Spearman's rank (*rho* = 0.863, p = 0.000) and Pearson correlation (R = 0.860, p = 0.000). The pH-$q_{u(ave)}$ yielded a fair and positive statistically significant Spearman's rank (*rho* = 0.451, p = 0.006) and Pearson correlation (R = 0.380, p = 0.022). Whereas a negative and statistically significant correlation on pH-*CD* was calculated through Spearman's rank (*rho* = -0.471, p = 0.003) and Pearson correlation (R = -0.468, p = 0.269), which supports the measured decrease of pH for all WA-WS specimens over 28 curing days (Fig. 9(a)). These findings suggest *WADR* contribution in promoting alkaline environment for soil binding. Particularly, low cementation is exhibited by 5% *WADR*, whereas at 15% and 25% WADR, the maximum strength is mobilized at 14 days. However, 15% *WADR* mixed soils exhibited a notable decrease in 28-day strength (Fig. 6) and stiffness (Fig. 8(a)). Conversely, at 25% *WADR*, the mixed soils maintained a high pH with a slight reduction in 28-day $q_{u(ave)}$ and better stiffness (Fig. 8(b)).

Notably, lime (or CaO-based) mixed soils exhibit a variation in the time period for the maximum strength mobilization, after which strength could remain constant or decrease (Thompson 1968, Okagbue 2007). Nevertheless, these findings suggest that WA dosage higher than 15% stimulates the effective release of SiO_2 (from Quartz) and Al_2O_3 (from Albite) constituents in WS (Keller 1955), which further contributes to the hydration reaction over curing days (Iler 1979, Pacheco-Torgal *et al*. 2008).

3.5 Total suction

The WA-WS soils in this study were exposed to unsaturated conditions and experienced WA hydration and concurrent pore water reduction. Thus, monitoring suction alteration in the mixtures during curing days is necessary. Fig. 10 plots the alteration of the measured gravimetric water contents (w_c) from the initial molding water contents and the total suction (Ψ), respectively, with WA contents and curing days. All specimens measured after UCS and total suctions tests exhibited an identical decrease in average w_c with an increase in WA contents over curing days, as shown in Fig. 10(a). Thus, it is assumed that the measured Ψ are equivalent for the specimens tested on the same days and WA rate. Subsequently, the measured 7 and 28-day Ψ are plotted in Fig. 10(b) and compared with Balagosa *et al.* (2023)'s research on the total suction of

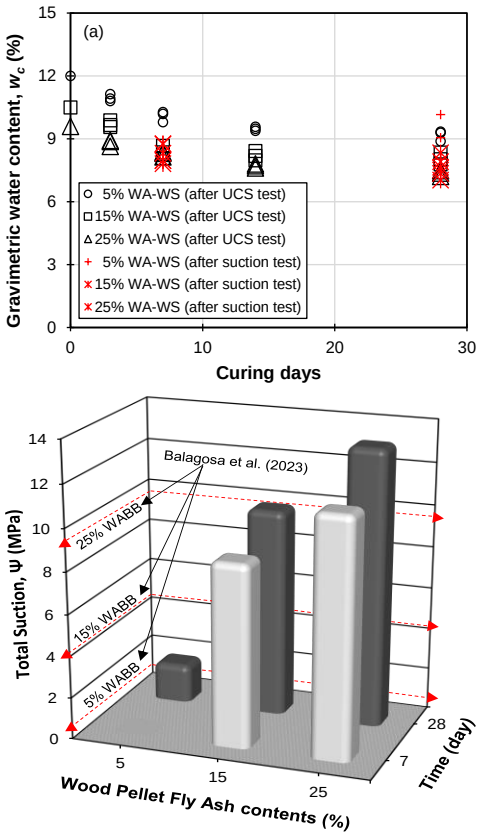

Fig. 10 Effects of WA contents and curing days on (a) measured w_c after UCS and suction test, and (b) total suction of WA-WS and compared to WABB stabilized WS (Balagosa *et al*. 2023)

wood pellet fly ash blended binder (WABB, a mixture of 50% WA, 30% ground granulated blast furnace slag, and 20% cement) treated WS, compacted at OMC and MDD (red dashed lines). The Ψ increases as WA dosage and curing day increase. In particular, the 28-day Ψ of 5% WA mixture specimen ranges from 1.69 to 1.94 MPa. The 7 and 28-day Ψ of 15%-WA samples are 8.57 and 10.3 MPa, respectively. The 25% WA-WS achieved Ψ ranges of 11.0 to 13.54 MPa. These findings suggests that the increase in Ψ is mainly contributed by the WA dosage rate.

The measured Ψ of WA-WS specimens is higher than those of unsaturated WABB stabilized WS specimens reported by Balagosa *et al*. (2023). These results suggest that pure WA generates fewer bridge connections and cementitious minerals in the WS matrix than WABB due to differences in binder ingredients. Muguda *et al*. (2017) proposed that the effectiveness of various cementitious binders on soil can be assessed through the production of hardened glassy-state microstructures. These modified soil particle contacts suggest a reduced in soil suction and yielding with a higher 28-day q_u and low Ψ. Notably, q_u fluctuations and sensitivity are based on the strength of the particle contact (Khan *et al*. 2006). Using the above analysis, the high Ψ of WA-WS is supported by a low 28-day q_u range 1.58 to 2.10 MPa than those of WABB-WS measured low Ψ with a 28-day q_u of 5.18 to 6.67 MPa. It is noteworthy, that these morphological change concurrently

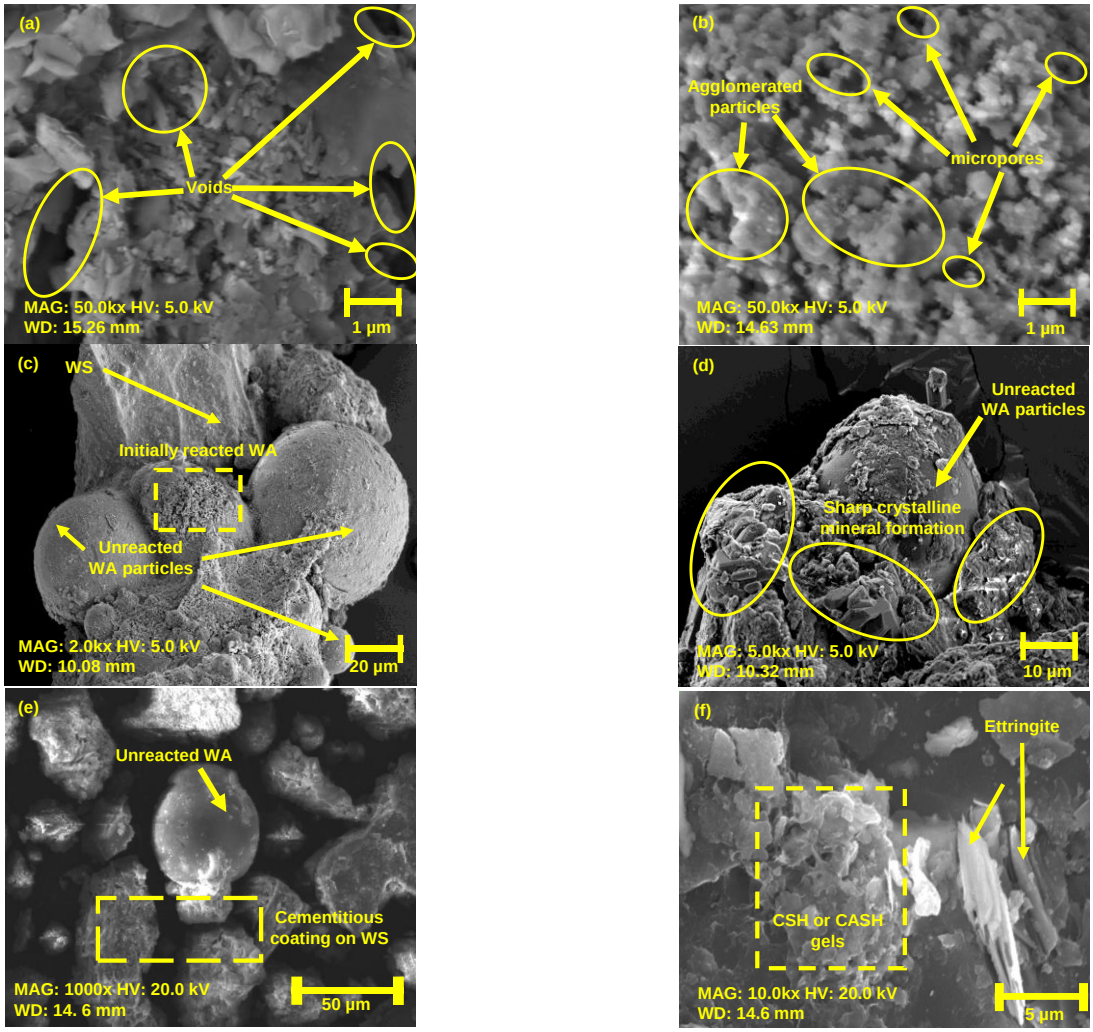

Fig. 11 SEM images of (a) WS at 1 µm; (b) WA at 1 µm; WA25-C14-1: (a) 20 µm (b) 10 µm; and WA25-C28-3: (c) 50 µm and (d) 5 µm (the selected areas with dashed lines were examined for elemental EDS analysis)

develop a pore size reduction with a tendency to retain and dry water particles under drying paths leading to increased suction (Jing *et al*. 2022, Lu and Likos 2004). The measured Ψ are based on the 2% to 3% desaturation from the OMC of WA-WS specimens over 28 curing days, and further studies are required to fully understand the hydraulic properties and the soil-water characteristic curves (SWCC) of compacted WA stabilized WS. Furthermore, the high measured Ψ of WA-WS and the coupled effects on the strength development will be discussed in the Section 4.2 Cementation and Suction Development.

4. Discussion

4.1 Microstructural analysis and investigation of cementation

SEM-EDS and XRD were employed to characterize the development of morphologies and microstructures of the 25%-WA specimens over curing time. These specimens were investigated due to their durability and sustained strength gain. Fig. 11 presents the SEM images on WS, WA, and compacted 25%-WA-treated specimens on the morphology at 14 and 28 curing days. Fig. 11(a) reveals the angular shapes and voids between the WS grains. These findings validate the low q_u and E_{50} of WS (Figs. 5 and 6, respectively) owing to its voids causing separation on the soil skeleton. WA shows irregular and agglomerated particles with micropore structure (Fig. 11(b)). These physical features are typical to biomass ash, owing to the biomass origin and combustion process, which in turn influence the ash's surface area and reactivity when used as binder (Thomas *et al*. 2021). The 14-day-cured sample shows an enormous amount of sharp crystalline minerals on the surface of grains (as shown in Figs. 11(c) and 11(d)). Whereas in the 28-day specimen, a reduction of sharp crystalline minerals suspected as ettringite (this mineral physical feature is previously introduced by Mehta, 1983) was observed (Figs. 11(e) and 11(f)). Additionally, the bulk surface of the WS particles is observed coated with flat coherent and dense surface layer minerals (Fig. 11(f)) suspected as calcium silicate hydrate (CSH) or calcium aluminum silicate hydrate (CASH) gels (these physical

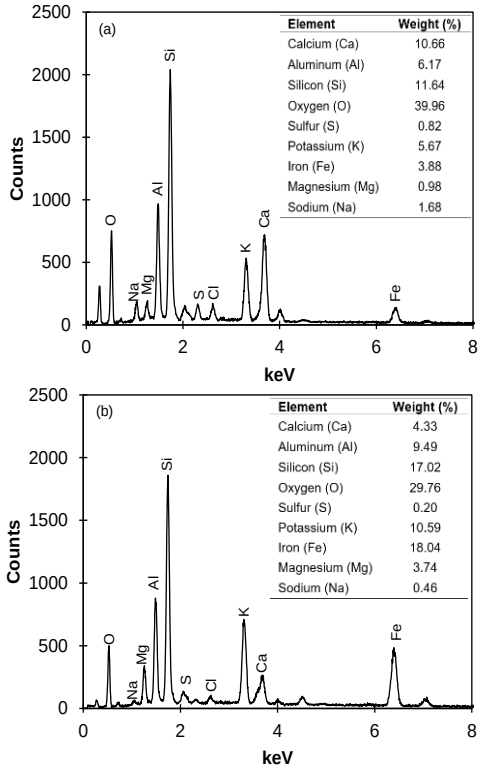

Fig. 12 EDS spectra on suspected cementitious minerals' morphology of WA25-C28-3 at: (a) 50 µm and (b) 5 µm

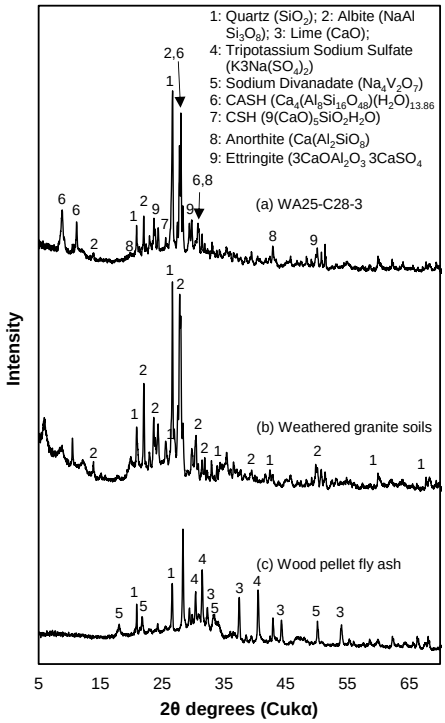

Fig. 13 X-ray diffraction patterns and scanning electron microscope of (a) WA25-C28-3, (b) weathered granite soils, and (c) wood pellet fly ash.

shape of the detected cementitious gels were also confirmed by Yi *et al.* 2014, Choobbasti and Kutanaei 2017). It is noteworthy that the observed morphology suggests progressive WA alkaline activation on the WS surface and a and a higher hydration reactivity to the silt-size particles of WS (Fig. 2). These small soil particles have a larger surface area that serves as ideal locations where binder cementation is more active (Yoon *et al.* 2020). Interestingly biomass ash soil binders with CaO constituents of 20% to 34% were observed to alter the soil particles of clay (Nath *et al.* 2018, Okagbue 2007), sand (Šķēls *et al.* 2016), and non-plastic silty sand (Cherian and Siddiqua 2021) over curing time. These suspected cementitious minerals are further evaluated through EDS to investigate their propensities.

Fig. 12 reveals that calcium (Ca), aluminum (Al), silicon (Si), and oxygen (O) are the most prevalent chemical elements (EDS analysis on the square spectrum with a dashed line in Figs. 11(e) and 11(f)). It is believed that CSH or CASH gel propensities are higher. Additionally, the detection of sulfur (S) indicates the emergence of ettringite minerals. These sharp crystalline minerals affect the strength gain and the development of the soil packing matrix (Wild *et al*. 1996). However, the low amount of sulfur ranging from 0.20 to 0.82, suggests low propensity of ettringite minerals, as observed in the 28-day morphologies. EDS also detected K, Fe, Na, and Mg confirming the alkaline contribution of WA to WS leading to a stronger soil-WA particle interaction (Kulanthaivel *et al*. 2022) with weathered granite soils and corroborating. Furthermore, the measured high pH of 25% WA-WS specimens helps facilitate the rapid release of soil silica and alumina which contributes to the development of the cementitious minerals (Puppala *et al*. 2003).

WA-WS cementation is further found by the XRD results shown in Fig. 13. Originally, the WS contained a majority of albite and quartz, which serves as additional source of alumina and silica. WA has quartz, lime, tripotassium sodium sulfate, and sodium divanadate. On the other hand, the peak intensity of albite and quartz within the stabilized WS (WA25-C28-3 in Fig. 13(a)) is observed to be lower than WS (as shown in Fig. 13(c)). In addition, new diffraction peaks of cementitious minerals such as CASH, CSH, anorthite, and ettringite were detected. The present study agrees with Sumesh *et al*. (2021)'s observation on the anorthite mineral's tendency to produce CSH with a propensity for infusion of CASH gels. On top of that, the present study confirms the contribution of albite minerals combined with cementitious binders in developing CSH and CASH gels (Tang *et al*. 2018, Jain *et al*. 2022). Interesting ly biomass ash soil binders with CaO constituents of 20% to 34% were observed to develop cementitious minerals such as CSH and CASH gels on clay (Nath *et al*. 2018, Okagbue 2007) and non-plastic silty sand (Cherian and Siddiqua 2021) over curing time. Hence, the CaO and alkali components of WA contributes to the development of these cementitious minerals that serve as a hardening source in improving the strength of the WA-WS over curing time.

4.2 Cementation and suction development

To analyze the strength-gaining mechanism provided by particle cementation and suction at 15% and 25% WA dosage, the rate of change of w_c, q_u, and ε_f over curing days are defined as follows

$$\Delta w_c\ (\%) = \left|\left(\frac{w_{c(i)}}{w_{c(m)}} - 1\right) \times 100\right| \quad (1)$$

$$\Delta q_{u(i)}\ (\%) = \left|\left(\frac{q_{u(i)}}{q_{u(3)}} - 1\right) \times 100\right| \quad (2)$$

$$\Delta \varepsilon_f\ (\%) = \left|\left(\frac{\varepsilon_{f(i)}}{\varepsilon_{f(3)}} - 1\right) \times 100\right| \quad (3)$$

where Δw_c is the rate of change of w_c, $w_{c(i)}$ is the measured water content at specified curing days, and $w_{c(m)}$ is the molding water content; $\Delta\varepsilon_f$ is the rate of change of ε_f, $\varepsilon_{f(i)}$ is the measured failure strain at a specified ith curing day, $\varepsilon_{f(3)}$ is the measured 3-day-ε_f representing the change in stiffness under minimal suction; Δq_{ui} is the rate of change of q_u, $q_{u(i)}$ is the measured strength at a specified ith curing day, $q_{u(3)}$ is the measured 3-day strength representing early strength with minimal suction. Fig.14 shows that Δw_c, $\Delta\varepsilon_f$, and Δq_u rapidly increase up to 14 days, then decrease at 28 days. In particular, the 7- and 14-day Δw_c of 15%WA-WS is 20.4% to 22.6% presenting higher moisture desorption than that of 25%WA-WS having Δw_c of 14.3% to 20%, respectively. Then the measured 28-day Δw_c for 15% and 25% WA-WS is almost identical and gradually decreasing. The measured rapid desaturation rate can be linked to the hydration of fresh cementitious materials and the influence of suction at early stage of curing (Abdul-Hussain and Fall 2011). Wherein these generated soil suctions increase the effective stress inside the soil matrix leading to the increase in soil strength (Witteman and Simms 2017). The development of $\Delta\varepsilon_f$ and Δq_u of WA-WS supports the contribution of WA alkaline activation on the change of WS particles contact over curing days. Both $\Delta\varepsilon_f$ and Δq_u of 15% WA and 25% WA specimens rapidly increase to 14 days, then decreases at 28 days. The higher $w_{c(m)}$ applied to 15% WA-WS serves as higher supply of water needed for WA hydration, thus resulting in an almost identical 14-day strength and moduli gain with 25% WA-WS. However, given theven the shortage on the availability of WA alkali components and CaO contents during hydration, adverse effects of shrinkage propagated. Hence, these behaviours were evidently shown by 15% WA-WS notable decrease on 28-day ε_f, q_u, and premature cementation of 5% WA-WS samples. Thus, these findings support the so-called short-lived strength gain for biomass ash-stabilized soils, especially at lower dosage rates (Okagbue 2007). On the other hand, the 25%WA-WS exhibited more sustained WA's activation on WS particles due to slight decrease on q_u and ε_f suggesting a higher presence of cementitious minerals. The unique stabilizing effect of a higher biomass dosage rate (20%) has been evidenced by the study of Šķēls *et al*. (2016) in stabilizing sandy soils.

WA-WS specimens exhibited higher Ψ, indicating that hydrogels formation on the WS surface (as shown in Fig. 11). Yet, WA has limited supply of cementitious chemicals, hence leading to lower quantities of cementitious minerals that could fill the inter and intra-aggregate pores in the WS matrix. As a result, WA may be characterized as BFA material that can generate cementitious minerals with low

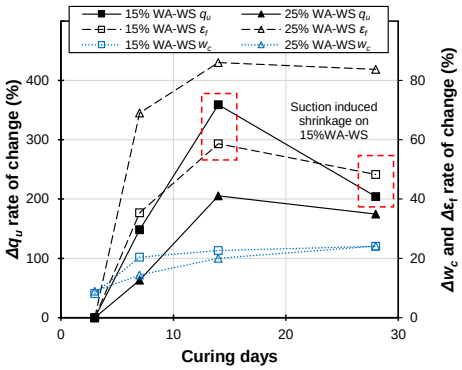

Fig. 14 Effects of wood pellet fly ash contents on the change of q_u and w_c of WA-WS samples over curing days

pore refinement capacity, as evidenced by its higher Ψ than WABB-WS (as shown in Fig. 10). Previous studies suggest the effect of suction on the strength gain of cementitious soils decreases as the curing days increase (Wang *et al.* 2017, Min *et al.* 2021, Jing *et al.* 2022, Wang *et al.* 2022), while suction is still discernible due to continuous binder hydration on soil (Abdul-Hussain and Fall 2011). However, this study focuses on the effect of WA's cementation and the improvement in WS particle density, and the influence of suction and hydraulic properties is out of this scope and further studies are needed. In addition, the stabilizing mechanism of WA were observed to contribute to the nonlinear relationships as displayed by $\Delta\varepsilon_f$, and Δq_u up to 28 days (Fig. 14). Using the above analyses, the association of *WADR*, *CD*, and 3-to-28-day unconfined compressive strength ($q_{u(3\ to\ 28)}$) and failure strain ($\varepsilon_{f(3\ to\ 28)}$) of on 15% and 25% WA-WS specimens were evaluated through Spearman's rank and Pearson correlation. A fair positive, statistically significant association between $q_{u(3\ to\ 28)}$-*CD* is indicated by Spearman's rank (*rho* = 0.412, p = 0.013) and Pearson correlation (R = 0.357, p = 0.033). Whereas the $q_{u(3\ to\ 28)}$-*WADR* showed a moderate positive statistically significant Spearman's rank (*rho* = 0.756, p = 0.000) and Pearson correlation (R = 0.716, p = 0.000).

A fair to moderate positive, statistically significant association between $\varepsilon_{f(3\ to\ 28)}$-*CD* and $\varepsilon_{f(3\ to\ 28)}$-*WADR* were indicated by Spearman's rank (*rho* = 0.620, p = 0.000; *rho* = 0.474, p = 0.004, respectively) and Pearson correlation (R = 0.567, p = 0.000; R = 0.572, p = 0.000, respectively). Notably the *rho* and R of $q_{u(3\ to\ 28)}$-*CD* and $\varepsilon_{f(3\ to\ 28)}$-*CD* is slightly lower. These findings suggest contribution of the time period for the maximum strength mobilization and the difference on the magnitudes of q_u decrease between WA-WS specimens (Fig. 14). Nevertheless, the association of *CD*, *WADR* with $q_{u(3\ to\ 28)}$ and $\varepsilon_{f(3\ to\ 28)}$ were positive and statistically significant. Following that, these parameters were utilized to develop empirical equations for $q_{u(3\ to\ 28)}$ and $\varepsilon_{f(3\ to\ 28)}$ of 15% and 25% WA-WS specimens. Initially, the 70% of the total data were divided for training while 30% for cross-validation to develop polynomial regression models. The results of the prediction models were compared and assessed using three criteria: *rho*, R, p, and the average absolute percentage error (AAPE) (Balagosa *et*

al. 2023, Gowida *et al.* 2021, Kim and Kim 2016), and depicted with Eqs. (4) and (5) as follows.

$$q_{u\,(3\ to\ 28)}\,(MPa) = -3.32 \times 10^{-3}\,WADR^2 + 161.82 \times 10^{-3}\,WADR + 32.66 \times 10^{-3}\,CD - 1022.64 \times 10^{-3} \quad (4)$$

$$(r^2 = 0.72)$$

$$\varepsilon_{f\,(3\ to\ 28)}\,(\%) = -1.62 \times 10^{-3}\,WADR^2 + 74.45 \times 10^{-3}\,WADR + 190.41 \times 10^{-3}\,CD - 413.6 \times 10^{-3} \quad (5)$$

$$(r^2 = 0.79)$$

As a result, the empirical Eqs. (4) and (5) present a moderate agreement between *WADR*, *CD*, $q_{u(3\ to\ 28)}$, and $\varepsilon_{f(3\ to\ 28)}$ is shown by their r^2 value of 0.72 and 0.79, as illustrated in Figs. 15(a) and 15(b). The predicted and measured q_u and ε_f values have a moderate positive and statistically significant as indicated by the calculated *rho*, *R*, and *p*. Notably, the high correlation coefficients (r^2 = 0.84 and 0.94) suggests that the model equations can be used as valuable technical tool for characterizing the relationship between mechanical and deformation properties of stabilized mixes (Wang *et al.* 2018). However, WA-WS specimens cured under various circumstances, such as submersion, freezing, heating, and so on may alter the r^2. Nevertheless, the obtained results can still be deemed appropriate for characterizing the quantitative correlation between q_u, ε_f, *WADR*, and *CD* in case of the absence of data. Then additional predictive model is proposed to fit the experimental results into a 3 to 28-day E_{50} ($E_{50(3\ to\ 28)}$) of WA-WS by normalizing the E_{50} and q_u of WA-WS with the strength and moduli of compacted WS without WA. As a result, the slope generated from the linear relationship of E_{50} with q_u (m = 1.64; r^2 = 0.96) was used for the E_{50} predictive model of WA-WS, as shown in Eq. (6)

$$E_{50\,(3\ to\ 28)}\,(MPa) = 1.64\left(\frac{q_{u(7\ to\ 28)WS-WA}}{q_{u(WS-AVE)}}\right) \times E_{50(WS-AVE)} \quad (6)$$

A good agreement between the model Eq. (6) and the experimental data illustrated in Fig. 15(c) suggesting strong support of WA strength and moduli correlations at dosage rates of 15% and 25%. Natural weathered granite soils possess an adverse or metastable structure wherein an increased imposed matric suction under partial saturation cause the weakening of inter-particle bonds (Lawton *et al.* 1992). Hence, the use of 15% WA (or greater) up to 25% WA may potentially reduce the adverse effects of suction and sustain the strength and durability of compacted WS. To maintain a more durable WA-WS matrix and is aided by WA's ability to form cementitious minerals (e.g., CSH, CASH, ettringite, anorthite). Therefore, the q_u, ε_f and E_{50} of compacted WS and $q_{u(7\ to\ 28)WA\text{-}WS}$ can be used to estimate the WA-WS' 7 to 28-day secant moduli. These parameters are essential for quality control and an in-depth monitoring of bearing capacity and deformation analysis in cases where solidified or stabilized soils are utilized as a bearing stratum

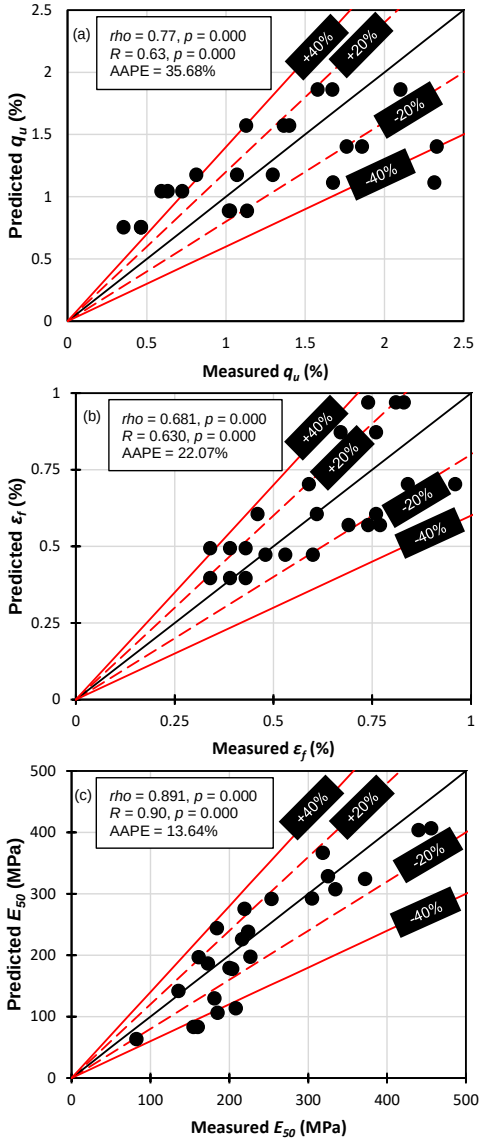

Fig. 15 Comparison of the 3 to 28-day predicted and measured: (a) q_u, (b) ε_f, and (c) E_{50} of 15% and 25% WA-WS

(Balagosa *et al.* 2023, Choobbasti and Kutanaei 2017, Wang *et al.* 2018).

Notably, the predictive models can only be used by adopting the target ρ_d and range of OMC (used in the present study) at 15% and 25% WA as dosage treatment. Also, the predicted models can be used to monitor the strength gain of partially saturated compacted WA-WS with a measured w_c desaturation of 2 to 3% from the OMC over 28 curing days. Regardless of some testing constraints and limitations in the current study, the experiment results and empirical formula are deemed to have provided vital information on the performance of the wood pellet fly ash and initial judgement for design although the effect of compaction is not considered in this study since the WA-WS specimens were prepared at a minimal range of ρ_d. Utilizing WA as a new construction material offers environmental and economic benefits, such as waste reduction, resource efficiency, and a lower carbon footprint.

The unique binding potential provided by WA in WS contributed to the improved stiffness and durability, while also offering economic advantages due to its availability at no expense from biomass power plants. Additionally, it promotes local economies by reducing the need for high-quality fill materials. However, it is imperative to evaluate challenges such as variable in composition of WA by-products, potential leaching of contaminants, and the need for comprehensive research loop on WA stabilized soils. Nevertheless, the findings of this study revealed a cost-effective way to improve the mechanical properties and microstructures of the alternative weathered granite soil backfill materials.

5. Conclusions

An experimental investigation was conducted to explore the potential enhancements of wood pellet fly ash on the mechanical properties and microstructures of compacted weathered granite soils. WA is mixed with the WS at various proportions to develop recycling technology and to produce an enhanced subgrade material used in backfill. For this purpose, several series of laboratory tests were performed on the compacted WA-WS mixtures to evaluate the geotechnical characteristics and improvements of the soil matrix. This resulted in the following conclusions:

• This study provides the first observation of the WA strength mobilization to WS. The WA's physicochemical interactions contributed to the alkaline environments on WS, by activating its silica and alumina constituents as seen by the early compaction properties.

• The WA-WS specimens displayed a maximum strength mobilization at 14 days. The most durable dosage rate is 25% WA mixtures, exhibiting a q_u and E_{50} increase of 7.18 and 12.37 times, respectively, than compacted WS without WA.

• New cementitious minerals such as CASH, CSH, anorthite, and ettringite were detected at 28 days. These minerals contributed to the strength gain and stiffness of WA-WS specimens.

• The strength developments of the unsaturated WA-WS specimens are influenced by total suction and cementation. WA's cementation contributes to the alteration of WS' fine micropores, which leads to the increase of total suction and q_u.

• The fitting parameters wood pellet fly ash dosage rate and curing days showed a strong association with changes in strength and stiffness. This association led to the development of polynomial equations for $q_{u(3\ to\ 28)}$, $\varepsilon_{f(3\ to\ 28)}$, and $E_{50(3\ to\ 28)}$ with satisfactory model performance. These model equations offer a sustainable solution for evaluating the performance of wood pellet fly ash stabilized weathered granite soils.

Future research should explore higher WA dosage rates, varying dry densities, broader range of water contents, and effects of elevated temperatures to enhance the robustness of the proposed models. Additionally, the influence of wide range of suction on strength gain with curing time, will provide insights into the hydromechanical properties of WA-WS mixtures. These varying testing conditions may contribute to the comprehensive understanding of strength mobilization of WA mixed WS.

This paper presents the application of pure WA on the mechanical properties of popular weathered soils. Possible combinations with additional agents are also planned to stabilize different type of soils and for field application to improve the performance for multi-purposes. These will allow for proposing a robust design framework for the usage of wood pellet fly ash to extend applicable fields.

Acknowledgments

This work was supported by the National Research Foundation of Korea (NRF) grant funded by the Korea government and Ministry of Science and ICT (MSIT) (No.2021R1A2C2009985).

References

AASHTO Transportation Officials (1993), *AASHTO Guide for Design of Pavement Structures*, **1**.

Abbasi, T. and Abbasi, S.A. (2010), "Biomass energy and the environmental impacts associated with its production and utilization", *Renew. Sust. Energ. Rev.*, **14**(3), 919-937. https://doi.org/10.1016/j.rser.2009.11.006.

Abdul-Hussain, N. and Fall, M. (2011), "Unsaturated hydraulic properties of cemented tailings backfill that contains sodium silicate", *Eng. Geol.*, **123**(4), 288-301. https://doi.org/10.1016/j.enggeo.2011.07.011.

ACI Committee 229 (1994), *Controlled Low Strength Materials (CLSM)*, ACI 229R-94: *Concrete Int*., **16**(7), 55-64.

Ale, T.O. (2023), "Improving the geotechnical properties of a Nigerian termite reworked soil using pretest drying conditions and sawdust ash", *Int. J. Geo-Eng.*, **14**(1), 1. https://doi.org/10.1186/s40703-022-00178-3.

Alhassan, M. (2008), "Potentials of Rice Husk Ash for Soil Stabilization", *Assumption University Journal of Technology, Bangkok, Thailand (AU)*, Bangkok, Thailand.

Ali, F.H., Adnan, A. and Choy, C.K. (1992), "Use of rice husk ash to enhance lime treatment of soil", *Can. Geotech. J.*, **29**(5), 843-852. https://doi.org/10.1139/t92-091.

Almajed, A., Dafalla, M. and Shaker, A.A. (2023)., "The combined effect of calcium chloride and cement on expansive soil materials", *Appl. Sci.*, **13**(8), 4811. https://doi.org/10.3390/app13084811.

Anupam, A.K., Kumar, P. and Ransinchung, G.D. (2013), "Use of various agricultural and industrial waste materials in road construction", *Procedia - Social and Behavioral Sciences*, **104**, 264-273. https://doi.org/10.1016/j.sbspro.2013.11.119.

ASTM D1557 (2012), *Standard Test Methods for Laboratory Compaction Characteristics of Soil Using Modified Effort (56,000ft-lbf/ft3(2,700 kN-m/m3))*, West Conshohocken, Pennsylvania, USA:

ASTM D2166 (2016), *Standard Test Method for Unconfined Compressive Strength of Cohesive Soil*, West Conshohocken, Pennsylvania, USA.

ASTM D2487 (2020), *Standard Practice for Classification of soils for Engineering Purposes (Unified Soil Classification System)*, West Conshohocken, Pennsylvania, USA.

ASTM D5239 (2012), *Standard Practice for Characterizing Fly*

Ash for Use in Soil Stabilization, West Conshohocken, Pennsylvania, USA.

ASTM D6913 (2017), *Standard Test Methods for Particle-Size Distribution (Gradation) of Soils Using Sieve Analysis*, West Conshohocken, Pennsylvania, USA.

Ayininuola, G.M. and Oyedemi, O.P. (2013), "Impact of hardwood and softwood ashes on soil geotechnical properties", *Trans. J. Sci. Tech. y*, **3**(10), 1-7.

Bagherinia, M. and Işik, N. (2022), "Investigation of physicochemical changes of soft clay around deep geopolymer columns", *Environ. Eng. Geosci.*, **28**(4), 371-386. https://doi.org/10.2113/EEG-D-21-00099.

Bagherinia, M. and Zaimoğlu, A.Ş. (2021), "Effect of deep chemical mixing columns on properties of surrounding soft clay", *Proceedings of the Institution of Civil Engineers - Ground Improvement*, **174**(2), 95-104. https://doi.org/10.1680/jgrim.18.00108.

Balagosa, J., Lee, M.J., Choo, Y.W., Kim, H.S. and Kim, J.M. (2023). "Experimental validation of the cementation mechanism of wood pellet fly ash blended binder in weathered granite soil", *Materials*, **16**(19), 6543. https://doi.org/10.3390/ma16196543.

Balagosa, J., Navea, I.J., Lee, M.J., Choo, Y.W., Kim, H.S. and Kim, J.M. (2024), "Dynamic property growth of weathered granite soils stabilized with wood pellet fly ash based binders", *Soil Dyn. Earthq. Eng.*, **180**, 108627, https://doi.org/10.1016/j.soildyn.2024.108627.

Barbosa, F.L. and Cordeiro, G.C. (2021), "Partial cement replacement by different sugar cane bagasse ashes: Hydration-related properties, compressive strength and autogenous shrinkage", *Constr. Build. Mater.*, **272**, 121625. https://doi.org/10.1016/j.conbuildmat.2020.121625.

Basha, E.A., Hashim, R., Mahmud, H.B. and Muntohar, A.S. (2005). "Stabilization of residual soil with rice husk ash and cement", *Constr. Build. Mater.*, **19**(6), 448-453, https://doi.org/10.1016/0.1016/j.conbuildmat.2004.08.001.

Behnood, A. (2018), "Soil and clay stabilization with calcium- and non-calcium-based additives: A state-of-the-art review of challenges, approaches and techniques", *Transport. Geotech.*, **17**, 14-32. https://doi.org/10.1016/j.trgeo.2018.08.002.

Bhatt, A., Priyadarshini, S., Acharath Mohanakrishnan, A., Abri, A., Sattler, M. and Techapaphawit, S. (2019), "Physical, chemical, and geotechnical properties of coal fly ash: A global review", *Case Studies Constr. Mater.*, **11**, e00263. https://doi.org/10.1016/j.cscm.2019.e00263.

Bohrn, G. and Stampfer, K. (2014), "Untreated wood ash as a structural stabilizing material in forest roads", *Croatian J. Forest Eng. : J. Theory Appl. Forestry Eng.*, **35**(1), 81-89.

Burke, B.C., Heimsath, A.M. and White, A.F. (2007), "Coupling chemical weathering with soil production across soil-mantled landscapes", *Earth Surface Processes and Landforms*, **32**(6), 853-873. https://doi.org/10.1002/esp.1443.

Butt, W.A., Gupta, K. and Jha, J.N. (2016), "Strength behavior of clayey soil stabilized with saw dust ash", *Int. J. Geo-Eng.*, **7**(1), 18. https://doi.org/10.1186/s40703-016-0032-9.

Chang, I., Im, J., Prasidhi, A.K. and Cho, G.C. (2015), "Effects of Xanthan gum biopolymer on soil strengthening", *Constr. Build. Mater.*, **74**, 65-72. https://doi.org/10.1016/j.conbuildmat.2014.10.026.

Cherian, C. and Siddiqua, S. (2021), "Engineering and environmental evaluation for utilization of recycled pulp mill fly ash as binder in sustainable road construction", *J. Cleaner Product.*, **298**, 126758. https://doi.org/10.1016/10.1016/j.jclepro.2021.126758.

Choobbasti, A.J. and Kutanaei, S.S. (2017), "Microstructure characteristics of cement-stabilized sandy soil using nanosilica", *J. Rock Mech. Geotech. Eng.*, **9**(5), 981-988. https://doi.org/10.1016/j.jrmge.2017.03.015.

Cohen, J. (1988), *Statistical Power Analysis for the Behavioral Sciences*, 2nd Ed., Routledge, New York.

Das, G., Razakamanantsoa, A., Herrier, G. and Deneele, D. (2022), "Influence of wetting fluids on the compressive strength, physicochemical, and pore-structure evolution in lime-treated silty soil subjected to wetting and drying cycles", *Transport. Geotech.*, **35**, 100798. https://doi.org/10.1016/j.trgeo.2022.100798.

Davidson, D.T. (1961), "Soil stabilization with lime fly ash", LIX. Iowa State University of Science and Technology & Highway Research Board.

Dayioglu, M., Cetin, B. and Nam, S. (2017), "Stabilization of expansive Belle Fourche shale clay with different chemical additives", *Appl. Clay Sci.*, **146**, 56-69. https://doi.org/10.1016/j.clay.2017.05.033.

Edil, T.B., Acosta, H.A. and Benson, C.H. (2006), "Stabilizing soft fine-grained soils with fly ash", *J. Mater. Civil Eng.*, **18**(2), 283-294. https://doi.org/10.1061/(ASCE)0899-1561(2006)18:2(283).

Etiégni, L. and Campbell, A.G. (1991), "Physical and chemical characteristics of wood ash", *Bioresource Technol.*, **37**(2), 173-178. https://doi.org/10.1016/0960-8524(91)90207-Z.

Farnsworth, C.B., Bartlett, S.F., Negussey, D. and Stuedlein, A.W. (2008), "Rapid construction and settlement behavior of embankment systems on soft foundation soils", *J. Geotech. Geoenviron. Eng.*, **134**(3), 289-301. https://doi.org/10.1061/(ASCE)1090-0241(2008)134:3(289).

Ferrari, A., Favero, V. and Laloui, L. (2013), "Experimental analysis of the retention behavior of shales", *Proceedings of the 47th US Rock Mechanics/Geomechanics Symposium*, USA.

Fořt, J., Šál, J., Ševčík, R., Doleželová, M., Keppert, M., Jerman, M., Záleská, M., Stehel, V. and Černý, R. (2021), "Biomass fly ash as an alternative to coal fly ash in blended cements: Functional aspects", *Constr. Build. Mater.*, **271**, 121544. https://doi.org/10.1016/j.conbuildmat.2020.121544.

Gidebo, F.A., Yasuhara, H. and Kinoshita, N. (2023), "Stabilization of expansive soil with agricultural waste additives: a review", *Int. J. Geo-Eng.*, **14**(1), 14. https://doi.org/10.1186/s40703-023-00194-x.

Gowida, A., Elkatatny, S. and Gamal, H. (2021), "Unconfined compressive strength (UCS) prediction in real-time while drilling using artificial intelligence tools", *Neural Comput. Appl.*, **33**(13), 8043-8054. https://doi.org/10.1007/s00521-020-05546-7.

Grau, F., Choo, H., Hu, J. and Jung, J. (2015), "Engineering behavior and characteristics of wood ash and sugarcane Bagasse ash", *Materials*, **8**(10), 6962-6977. https://doi.org/10.3390/ma8105353.

Greenberg, S.A. (1961), "Reaction between silica and calcium hydroxide solutions, I: kinetics in the temperature range 30 to 85°C", *J. Phys. Chem.*, **65**, 12-16.

Hawkins Wright (2017), 2017 wood pellet market outlook. Hawking Wright Ltd, United Kingdom. https://www.hawkinswright.com/news-and-events/blog/post/hawkins-wright-blog/2017/01/20/2017-wood-pellet-market-outlook.

Ho, L.S., Nakarai, K., Ogawa, Y., Sasaki, T. and Morioka, M. (2017), "Strength development of cement-treated soils: Effects of water content, carbonation, and pozzolanic reaction under drying curing condition", *Constr. Build. Mater.*, **134**, 703-712, https://doi.org/10.1016/j.conbuildmat.2016.12.065.

Holm, G. (2003), "State of practice in dry deep mixing methods", *3rd Int. Specialty Conf. on Grouting and Ground Treatment*, ASCE, Reston, VA, 145-163.

Horpibulsuk, S., Phetchuay, C., Chinkulkijniwat, A. and Cholaphatsorn, A. (2013), "Strength development in silty clay stabilized with calcium carbide residue and fly ash", *Soils Found.*, **53**(4), 477-486.

https://doi.org/10.1016/j.sandf.2013.06.001.
Iler, K.R. (1979), *The chemistry of silica. Solubility, polymerization, colloid and surface properties and biochemistry of silica*. Wiley, Hoboken, NJ, USA.
International Organization for Standardization (ISO) (2021), *ISO 17225-1:2021 - Solid biofuels — Fuel specifications and classes — Part 1: General requirements*. Geneva, Switzerland.
Jain, A., Chaudhary, S. and Gupta, R. (2022), "Mechanical and microstructural characterization of fly ash blended self-compacting concrete containing granite waste", *Constr. Build. Mater.*, **314**, 125480. https://doi.org/10.1016/j.conbuildmat.2021.125480.
Jing, P., Song, X., Zhang, J. and Nowamooz, H. (2022), "A review of hydro-mechanical coupling behaviour of cement-treated materials", *Constr. Build. Mater.*, **322**, 126446. https://doi.org/10.1016/j.conbuildmat.2022.126446.
Keller, W.D. (1955), *The principles of chemical weathering: Soil Science*, Lucas Brothers, Baltimore, MD, USA.
Khan, Z., Majid, A., Cascante, G., Hutchinson, D.J. and Pezeshkpour, P. (2006), "Characterization of a cemented sand with the pulse-velocity method", *Can. Geotech. J.*, **43**(3), 294-309. https://doi.org/10.1139/t06-008.
Kim, J.M., Choo, Y.W., Kim, H.S., Kang, I.G., Kim, G.W., Kim, B.S., Balagosa, J., Bae, G.H., Yun, J.S., Lee, M.J., Choi, J.H. and Ra, J.M. (2021a), "Development of non-cement based soil stabilizer using wood pellet fly ash", Final research report (project No. 2020-Field-01), Korea South-East Power Co, Jinju-si, Republic of Korea. (In Korean).
Kim, H.S., Kang, I.K., Shin, S.C. and Kim, J.M. (2021b), "Properties of CLSM Using Wood Pellets Fly Ash (in Korean)", *Proceedings of the Korean Recycled Construction Resource Institute 2021 Fall Conference*, 7-8. https://rcr.or.kr/publication/publication03_list.asp. (In Korean).
Kim, S. and Kim, H. (2016), "A new metric of absolute percentage error for intermittent demand forecasts", *Int. J. Forecast.*, **32**(3), 669-679. https://doi.org/10.1016/j.ijforecast.2015.12.003.
Kim, H.S., Kim, K.S. and Kim, Y.W. (2022), "Characteristics of solidification using wood pellets fly ash", *Proceedings of the Korean Recycled Construction Resource Institute 2022 Fall Conference*, 225-226. https://rcr.or.kr/publication/publication03_list.asp. (In Korean)
Kim, H.S., Park, J.H., Shin, S.C. and Kim, J.M. (2021c), "Properties of non-cement matrix using wood pellets fly ash (in Korean)", *Proceedings of the Korean Recycled Construction Resource Institute 2021 Spring Conference*, **21**, 3-4. https://www.auric.or.kr/User/Rdoc/DocRdoc.aspx?returnVal=RD_R&dn=405500. (In Korean).
Kulanthaivel, P., Soundara, B., Selvakumar, S. and Das, A. (2022), "Effect of bio-cementation on the strength behaviour of clay soils using egg shell as calcium source", *Environ. Earth Sci.*, **81**(13), 348. https://doi.org/10.1007/s12665-022-10475-w.
Lawton, E.C., Fragaszy, R.J. and Hetherington, M.D. (1992), "Review of wetting-induced collapse in compacted soil", *J. Geotech. Eng.*, **118**(9), 1376-1394. https://doi.org/10.1061/(ASCE)0733-9410(1992)118:9(1376).
Liu, Z., Deng, P. and Zhang, Z. (2022), "Application of silica-rich biomass ash solid waste in geopolymer preparation: A review", *Constr. Build. Mater.*, **356**, 129142. https://doi.org/10.1016/j.conbuildmat.2022.129142.
Lorenzo, G.A. and Bergado, D.T. (2006), "Fundamental characteristics of cement-admixed clay in deep mixing", *J. Mater Civil Eng.*, **18**(2), 161-174. https://doi.org/10.1061/(ASCE)0899-1561(2006)18:2(161).
Lu, N. and Likos, W. (2004), *Unsaturated Soil Mechanics*, Wiley, Hoboken, NJ, USA.
Ma, Y., Nie, Q., Xiao, R., Hu, W., Han, B., Polaczyk, P.A. and Huang, B. (2020), "Experimental investigation of utilizing waste flue gas desulfurized gypsum as backfill materials", *Constr. Build. Mater.*, **245**, 118393. https://doi.org/10.1016/j.conbuildmat.2020.118393.
Mácsik, J., Edeskär, T., Rogbeck, Y. and Ribbing, C. (2012), Stabilization of road structures with fly ash as binder component – through demo projects to full scale use, *ASH 2012*, Stockholm, Sweden.
Madhyannapu, R.S., Puppala, A.J., Nazarian, S. and Yuan, D. (2010), "Quality assessment and quality control of deep soil mixing construction for stabilizing expansive subsoils", *J. Geotech. Geoenviron. Eng.*, **136**(1), 119-128. https://doi.org/10.1061/(ASCE)GT.1943-5606.0000188.
Maeda, N., Katakura, T., Fukasawa, T., Huang, A.-N., Kawano, T. and Fukui, K. (2017), "Morphology of woody biomass combustion ash and enrichment of potassium components by particle size classification", *Fuel Process. Tech.*, **156**, 1-8. https://doi.org/10.1016/j.fuproc.2016.09.026.
Mehta, P.K. (1983), "Mechanism of sulfate attack on portland cement concrete — Another look", *Cement Concrete Res.*, **13**(3), 401-406. https://doi.org/10.1016/0008-8846(83)90040-6.
Mekonnen, E., Amdie, Y., Etefa, H., Tefera, N. and Tafesse, M. (2022), "Stabilization of expansive black cotton soil using bioenzymes produced by ureolytic bacteria", *Int. J. Geo-Eng.*, **13**(1), 10. https://doi.org/10.1186/s40703-022-00175-6.
Mimini, V., Sykacek, E., Syed Hashim, S.N.A., Holzweber, J., Hettegger, H., Fackler, K., Potthast, A., Mundigler, N. and Rosenau, T. (2019). "Compatibility of kraft lignin, organosolv lignin and lignosulfonate with PLA in 3D printing", *J. Wood Chem. Tech.*, **39**(1), 14-30. https://doi.org/10.1080/02773813.2018.1488875.
Min, C., Shi, Y. and Liu, Z. (2021), "Properties of cemented phosphogypsum (PG) backfill in case of partially substitution of composite Portland cement by ground granulated blast furnace slag", *Constr. Build. Mater.*, **305**, 124786. https://doi.org/10.1016/j.conbuildmat.2021.124786.
Ministry of Trade, Industry and Energy (2017a), 8th Basic Plan for Long-term Electricity Supply and Demand (BPLE) (2017 - 2031) | ESCAP Policy Documents Management. https://policy.asiapacificenergy.org/node/3844.
Ministry of Trade, Industry and Energy (2017b), Korea Renewable Energy 3020 Plan – Policies: IEA. https://www.iea.org/policies/6569-korea-renewable-energy-3020-plan.
Misra, M.K., Ragland, K.W. and Baker, A.J. (1993), "Wood ash composition as a function of furnace temperature", *Biomass Bioenergy*, **4**(2), 103-116, https://doi.org/10.1016/0961-9534(93)90032-Y.
Muguda, S., Booth, S.J., Hughes, P.N., Augarde, C.E., Perlot, C., Bruno, A.W. and Gallipoli, D. (2017), "Mechanical properties of biopolymer-stabilised soil-based construction materials", *Géotechnique Lett.*, **7**(4), 309-314. https://doi.org/10.1680/jgele.17.00081.
Murray, I. and Tarantino, A. (2019), "Mechanisms of failure in saturated and unsaturated clayey geomaterials subjected to (total) tensile stress", *Géotechnique*, **69**(8), 701-712. https://doi.org/10.1680/jgeot.17.P.252.
Narmluk, M. and Nawa, T. (2014), "Effect of curing temperature on pozzolanic reaction of fly ash in blended cement paste", *Int. J. Chem. Eng. Appl.*, **5**(1), 31-35. https://doi.org/10.7763/IJCEA.2014.V5.346.
Nath, B.D., Sarkar, G., Siddiqua, S., Rokunuzzaman, Md. and Islam, Md.R. (2018), "Geotechnical properties of wood ash-based composite fine-grained soil", *Adv. Civil Eng.*, **2018**, 1-7. https://doi.org/10.1155/2018/9456019.
Nunes, L.J.R., Matias, J.C.O. and Catalão, J.P.S. (2014), "A review on torrefied biomass pellets as a sustainable alternative to coal in power generation", *Renew. Sust. Energ. Rev.s*, **40**,

153-160. https://doi.org/10.1016/j.rser.2014.07.181.
Obrzud, R. and Truty, A. (2010), The hardening soil model - a practical guidebook. Zace services.
Oh, J. H., Hwang, J.S. and Cha, D.S. (2014), "Fuel Properties of Woody Pellets in Domestic Markets
of Korea", *J. Forest Environ. Sci.*, **30**(4), 362-369. https://doi.org/10.7747/JFES.2014.30.4.362.
Ojuri, O.O. and Epe, G.G. (2016), "Strength and leaching characteristics of crude oil contaminated sandy soil stabilized with sawdust ash-cement", *In Geo Chicago 2016 American Society of Civil Engineers*, 582-590.
Okagbue, C.O. (2007), "Stabilization of clay using woodash", *J. Mater. Civil Eng.*, **19**(1), 14-18. https://doi.org/10.1061/(ASCE)0899-1561(2007)19:1(14).
Opukumo, A.W., Davie, C.T., Glendinning, S. and Oborie, E. (2022). "A review of the identification methods and types of collapsible soils", *J. Eng. Appl. Sci.*, **69**(1), 17. https://doi.org/10.1186/s44147-021-00064-2.
Osinubi, K., Edeh, J. and Onoja, W. (2012), "Sawdust ash stabilization of reclaimed asphalt pavement", *J. ASTM Int.*, **9**. https://doi.org/10.1520/STP154020120022.
Otoko, G.R. and Honest, B.K. (2014), "Stabilization of Nigerian deltaic laterites with saw dust ash", *Int. J. Scientific Res. Management*, **2**(8), 1287-1292. https://doi.org/10.13140/2.1.4369.2805.
Pacheco-Torgal, F., Castro-Gomes, J. and Jalali, S. (2008), "Alkali-activated binders: A review: Part 1. Historical background, terminology, reaction mechanisms and hydration products", *Constr. Build. Mater.*, **22**(7), 1305-1314. https://doi.org/10.1016/j.conbuildmat.2007.10.015.
Phan, N.B., Hayano, K., Mochizuki, Y. and Yamauchi, H. (2021), "Mixture design concept and mechanical characteristics of PS ash–cement-treated clay based on the water absorption and retention performance of PS ash", *Soils Found.*, **61**(3), 692-707. https://doi.org/10.1016/j.sandf.2021.02.006.
Ponzoni, E., Nocilla, A. and Jommi, C. (2021), "Determination of water retention properties of silty sands by means of combined commercial techniques", *Geosci.*, **11**(8), 315. https://doi.org/10.3390/geosciences11080315.
Proskurina, S., Junginger, M., Heinimö, J., Tekinel, B. and Vakkilainen, E. (2019), "Global biomass trade for energy— Part 2: Production and trade streams of wood pellets, liquid biofuels, charcoal, industrial roundwood and emerging energy biomass", *Biofuels, Bioproducts and Biorefining*, **13**(2), 371-387. https://doi.org/10.1002/bbb.1858.
Puppala, A.J., Wattanasanticharoen, E. and Punthutaecha, K. (2003), "Experimental evaluations of stabilisation methods for sulphate-rich expansive soils", *Proceedings of the Institution of Civil Engineers - Ground Improvement*, **7**(1), 25–35. https://doi.org/10.1680/grim.2003.7.1.25.
Regasa, H., Jothimani, M. and Oyda, Y. (2023). "Subgrade soil stabilization using the Quicklime: a case study from Modjo-Hawassa highway, Central Ethiopia", *Int. J. Geo-Eng.*, **14**(1), 17. https://doi.org/10.1186/s40703-023-00197-8.
Roy, A. (2014), "Soil stabilization using rice husk ash and cement", *Int. J. Civil Eng. Res*., **5**(1), 49-54.
Sabat, A. and Nanda, R. (2011), "Effect of marble dust on strength and durability of Rice husk ash stabilised expansive soil", *Int. J. Civil Struct. Eng.*, **1**.
Sarkkinen, M., Kujala, K., Kemppainen, K. and Gehör, S. (2018), "Effect of biomass fly ashes as road stabilisation binder", *Road Mater. Pavement Des*., **19**(1), 239-251. https://doi.org/10.1080/14680629.2016.1235508.
Šķēls, P., Bondars, K., Plonis, R., Haritonovs, V. and Paeglītis, A. (2016), "Usage of wood fly ash in stabilization of unbound pavement layers and soils", *Proceedings of the 13th Baltic Sea Geotechnical Conference*, Vilnius Gediminas Technical University, Lithuania.
Sukmak, P., Kunchariyakun, K., Sukmak, G., Horpibulsuk, S., Kassawat, S. and Arulrajah, A. (2019), "Strength and microstructure of palm oil fuel ash–fly ash–soft soil geopolymer masonry units", *J. Mater. Civil Eng.*, **31**(8), 04019164. https://doi.org/10.1061/(ASCE)MT.1943-5533.0002809.
Sukprasert, S., Hoy, M., Horpibulsuk, S., Arulrajah, A., Rashid, A.S.A. and Nazir, R. (2021), "Fly ash based geopolymer stabilisation of silty clay/blast furnace slag for subgrade applications", *Road Mater. Pavement Des.*, **22**(2), 357-371. https://doi.org/10.1080/14680629.2019.1621190.
Sumesh, M., Alengaram, U.J., Jumaat, M.Z., Mo, K.H., Singh, R., Nayaka, R.R. and Srinivas, K. (2021), "Chemo-physico-mechanical characteristics of high-strength alkali-activated mortar containing non-traditional supplementary cementitious materials", *J. Build. Eng.*, **44**, 103368. https://doi.org/10.1016/j.jobe.2021.103368.
Tang, W.C., Wang, Z., Liu, Y. and Cui, H.Z. (2018), "Influence of red mud on fresh and hardened properties of self-compacting concrete", *Constr. Build. Mater.*, **178**, 288-300. https://doi.org/10.1016/j.conbuildmat.2018.05.171.
Thomas, B.S., Yang, J., Mo, K.H., Abdalla, J.A., Hawileh, R.A. and Ariyachandra, E. (2021), "Biomass ashes from agricultural wastes as supplementary cementitious materials or aggregate replacement in cement/geopolymer concrete: A comprehensive review", *J. Build. Eng.*, **40**, 102332. https://doi.org/10.1016/j.jobe.2021.102332.
Thompson, M.R. (1968), "Lime-treated soils for pavement construction", *J. Highway Division*, **94**(2), 191-217. https://doi.org/10.1061/JHCEA2.0000274.
Timoney, M.J., McCabe, B.A. and Bell, A.L. (2012), "Experiences of dry soil mixing in highly organic soils", *Proceedings of the Institution of Civil Engineers - Ground Improvement*, **165**(1), 3-14. https://doi.org/10.1680/grim.2012.165.1.3.
Vanhanen, H., Dahl, O. and Joensuu, S. (2014), "Utilization of wood ash as a road construction material - Sustainable use of wood ashes", *Sustain. Environ. Res.*, **24**(6), 457-465.
Wang, F., Li, K. and Liu, Y. (2022), "Optimal water-cement ratio of cement-stabilized soil", *Constr. Build. Mater.*, **320**, 126211. https://doi.org/10.1016/j.conbuildmat.2021.126211.
Wang, G., Shen, L. and Sheng, C. (2012), "Characterization of biomass ashes from power plants firing agricultural residues", *Energ. Fuel.*, **26**(1), 102-111. https://doi.org/10.1021/ef201134m.
Wang, Y., Wu, A., Wang, S., Wang, H., Yang, L., Wang, Y. and Ruan, Z. (2017), "Correlative mechanism of hydraulic-mechanical property in cemented paste backfill", *J. Wuhan Univ. Tech. Mater. Sci. Ed.*, **32**(3), 579–585. https://doi.org/10.1007/s11595-017-1637-3.
Wang, D., Zentar, R. and Abriak, N.E. (2018), "Durability and swelling of solidified/stabilized dredged marine soils with class-F fly ash, cement, and lime", *J. Mater. Civil Eng*., **30**(3), 04018013. https://doi.org/10.1061/(ASCE)MT.1943-5533.0002187.
Wild, S., Kinuthia, J.M., Robinson, R.B. and Humphreys, I. (1996), "Effects of ground granulated blast furnace slag (GGBS) on the strength and swelling properties of lime-stabilized kaolinite in the presence of sulphates", *Clay Minerals*, **31**(3), 423-433. https://doi.org/10.1180/claymin.1996.031.3.12.
Witteman, M.L. and Simms, P.H. (2017), "Unsaturated flow in hydrating porous media with application to cemented mine backfill", *Can. Geotech. J.*, **54**(6), 835-845 https://doi.org/10.1139/cgj-2015-0314.
Wood Resources International (2017), South Korea, Japan wood pellet imports near records in late 2016 |Biomassmagazine.com. https://biomassmagazine.com/articles/14481/south-korea-japan-wood-pellet-imports-near-records-in-late-2016.

Yi, Y., Liska, M. and Al-Tabbaa, A. (2014), "Properties of two model soils stabilized with different blends and contents of GGBS, MgO, lime, and PC", *J. Mater Civil Eng.*, **26**(2), 267-274. https://doi.org/10.1061/(ASCE)MT.1943-5533.0000806.

Yi, Y., Liska, M., Jin, F. and Al-Tabbaa, A. (2016), "Mechanism of reactive magnesia – ground granulated blastfurnace slag (GGBS) soil stabilization", *Can. Geotech. J.*, **53**(5), 773-782. https://doi.org/10.1139/cgj-2015-0183.

Yoon, B., Lee, W., Lee, C. and Choo, H. (2020), "Time-dependent variations of compressive strength and small-strain stiffness of sands grouted with microfine cement", *J. Geotech. Geoenviron. Eng.*, **146**(4), 06020001. https://doi.org/10.1061/(ASCE)GT.1943-5606.0002207.

Yuan, S., Liu, X. and Buzzi, O. (2021), "A microstructural perspective on soil collapse", *Géotechnique*, **71**(2), 132-140. https://doi.org/10.1680/jgeot.18.P.256.

Zivari, A., Siavoshnia, M. and Rezaei, H. (2023), "Effect of lime-rice husk ash on geotechnical properties of loess soil in Golestan province, Iran", *Int. J. Geo-Eng.*, **14**(1), 20. https://doi.org/10.1186/s40703-023-00199-6.

IC